*Eur. J. Mech. B - Fluids 19 (2000) 269–283*

S0997-7546(00)00104-7/FLA

# Open-channel flows and waterfalls

Fabrice Toison, Jacques Hureau *

*Laboratoire de Mécanique et d'Energétique, Ecole Supérieure de l'Energie et des Matériaux, Université d'Orléans, Rue Léonard de Vinci, 45072 Orleans cedex 2, France*

(Received 8 June 1999; revised and accepted 27 September 1999)

**Abstract** – Steady two-dimensional free-surface flows of an inviscid incompressible fluid are studied here, using the complex potential theory. The first flow is a uniform free stream flow in a channel of finite depth. The second is similar, but terminated abruptly as a downstream flow exiting into a falling jet, with and without the effect of gravity. These problems have already been solved for polygonal walls. This paper presents an iterative process for computing flows over arbitrarily shaped channels, with and without the presence of a waterfall at the exit. This process is based on the solution of a mixed boundary problem in the unit disk. The method emphasizes the correspondence between the walls in the physical plane and in the unit disk. The numerical data agree with previously published results and extend them to arbitrary curved walls. This method yields solutions only for supercritical flows. © 2000 Éditions scientifiques et médicales Elsevier SAS

**waterfall / mixed bounds problem / supercritical flow**

## 1. Introduction

Free streamline flows of an ideal fluid are essentially nonlinear problems, because of the Bernoulli's equation on the free surface. This is why, until the hodograph method introduced by Kirchhoff [1], very little progress on this type of fluid mechanics problems was made. Then, the limitations of this method emerged, since only walls constituted of polygons of very simple shape could be considered [2].

New means of calculation have given a new start to these studies, by providing the numerical integration of the Schwarz–Christoffel transformation. By the use of a modified Schwarz–Christoffel transformation, Dias, Elcrat and Trefethen [3] presented a numerical solution to jet and free streamline problems (weightless fluid). They considered either linear walls (polygons) or curved walls approximated by polygonal lines. Then, other methods were developed, where the free surface and the flow of the fluid were determined numerically either by series truncation or by using an integro-differential equation. It was then applied to the flow over an obstruction in a channel, this being a semi-circular obstacle (Forbes and Schwartz [4], Vanden-Broeck [5]) or a triangular obstacle (Dias and Vanden-Broeck [6]). The last method was also applied to the flow over a flat bottom ending in a vertical wall (Dias and Tuck [7]). In parallel, Bloor [8] gave a generalization of this Schwarz–Christoffel transformation, which transforms a half-plane into a region using both polygonal lines and smooth curves. This method was then applied to the flow over a step [9], and over a curved wall whose equation is given (weightless fluid [10] and heavy fluid [11]). A similar method has been presented by Peng and Parker [12], concerning the study of the impact of a jet against a curved wall (the equation of the wall being given again).

We present here an iterative method to compute the free streamline flow of a heavy fluid over a wall whose shape is arbitrary. The improvement of our method is to overcome both difficulties: it can take into account a

* Correspondence and reprints; e-mail: Jacques.Hureau@univ-orleans.fr

heavy fluid, and any curved wall is considered (its equation known or unknown). Following Dias, Elcrat and Trefethen, our method, first used for flows around obstacles with thick wakes [13,14], was then applied to flows over arbitrary obstacles, the impinging jet being an unbounded flow, a jet or a semi-infinite stream [15], and to the impact of two jets [16].

As Forbes [17] pointed it out, fixed-point methods cannot converge when the flow is subcritical, which explains the fact that only supercritical flows will be considered in this paper.

Section 2 introduces the notations and outlines our treatment. In Section 3, the boundary problem required for our method is presented. Section 4 presents the equations and an algorithm. Section 5 presents numerical results and comparisons and gives details about the numerical treatment.

## 2. Problem formulation

Two steady, irrotational, two-dimensional flows of an incompressible inviscid fluid are considered in *figure 1*. Thus the mathematical task will be described in terms of determining suitable analytical functions of complex variables. As their treatment makes use of the same solution method, we will only detail the study of OCF.

In the case of OCF, we consider a channel of arbitrary shape, submerged in an inviscid fluid tending toward a uniform upstream flow (*figure 1*, point A), where the velocity and depth are denoted $V_A$ and $H$, respectively. Point B is the origin of the curvilinear abscissa $s$, and will be generally chosen at the maximum channel bottom elevation. The pressure above the free surface, denoted by $P_0$, is assumed to be constant.

In the case of WF, the bottom of the channel ends at B (*figure 1*, right side) and consequently, with the heavy fluid hypothesis, the jet will be distorted downward by gravity and will eventually fall in an ever-tapering sheet. Far upstream, the flow tends to be the same as for OCF. For both problems, solutions will be fully determined when all streamlines are known, and particularly the free-surface line.

It is appropriate to define the Froude number:

$$F = \frac{V_A}{\sqrt{gH}}.$$

Then, the classical flows in the absence of gravity are just the limits as $F$ approaches infinity, and can be approximated in high-speed situations.

The usual hypothesis allows the existence of a complex potential, $f = \varphi + i\psi$, and of a complex velocity, $w = u - iv = \frac{df}{dz}$, with $z$ being the physical variable $x + iy$ and $u$, $v$ the components of the velocity.

Once both $f$ and $w$ are known, the flow domain $D_z$ in the physical plane $(z)$ is no longer unknown, and the relation $z = \int \frac{df}{w}$ gives the free surfaces in $D_z$. To express $w$ and $f$, then, we map $D_f$ and $D_w$ (potential domain and complex velocity domain respectively) conformally onto the same domain $D_\zeta$, with $(\zeta)$ being an auxiliary plane.

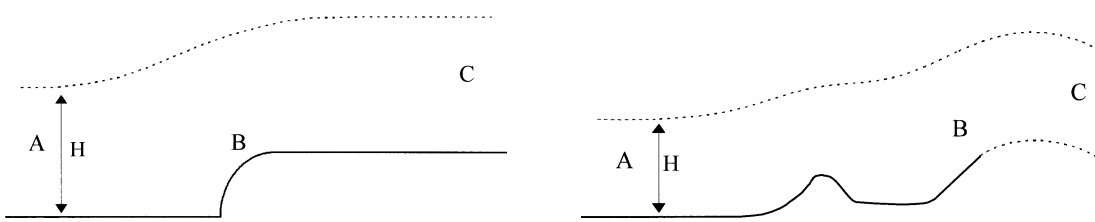


**Figure 1.** The flows considered, left: Open Channel Flow (OCF); right: Waterfall Flow (WF).

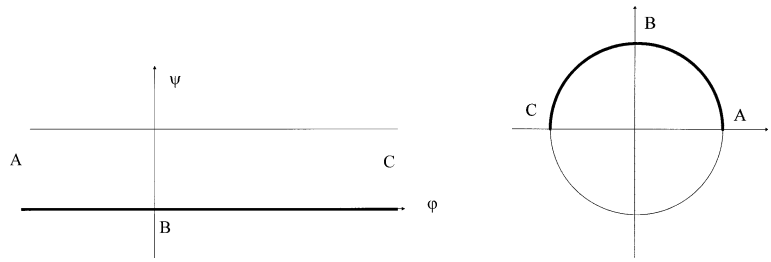


**Figure 2.** Conformal mapping of $D_f$ onto $D_\zeta$.

As $D_w$ is generally complicated, Kirchhoff introduced the Log-hodograph function $Q = \mathrm{Log}\frac{V_{\mathrm{ref}}}{w}$ (or $\Omega = i\mathrm{Log}\frac{w}{V_{\mathrm{ref}}}$), with $V_{\mathrm{ref}}$ being a reference velocity. The advantage of doing this lies in the fact that both variables $Q$ and $\Omega$ exhibit a real part and an imaginary part that depend only on the norm or argument of $w$, which means that:

– $|w|$ will be known on a streamline at constant pressure (i.e. free streamline when gravity is neglected),
– $\arg(w)$ will be known on a plane portion of wetted wall, due to the slip condition.

Therefore $D_Q$ or $D_\Omega$ is a polygon when polygonal walls are considered.

In this paper, our aim is to consider any arbitrary shape of wetted walls, and therefore $D_Q$ (or $D_\Omega$) are unknown. Nevertheless, the choice of $Q$ (or $\Omega$) remains relevant: both the imaginary and real parts of the Log-hodograph function will be specified alternately on the boundary of $D_\zeta$. Our task is now to determine $Q$ (or $\Omega$) from these conditions on the boundaries of $D_\zeta$. The initial problem of finding $w$ has been altered in order to determine $Q$ (or $\Omega$), by solving a boundary problem called the mixed problem, presented in the following section.

The boundary conditions can be expressed here:

$$\begin{cases} P = P_0 \quad \text{on the free surface AC,} \\ \mathrm{Im}(w \cdot \mathrm{d}z) = 0 \quad \text{on the wall ABC,} \\ |w| = V_{\mathrm{A}} \quad \text{far upstream.} \end{cases}$$

The conformal mapping of $D_f$ onto $D_\zeta$ is (*figure 2*):

$$f(\zeta) = \frac{V_{\mathrm{A}} H}{\pi} \mathrm{Log}\left( \frac{\frac{i-\zeta}{1-i\zeta} + 1}{\frac{i-\zeta}{1-i\zeta} - 1} \right).$$

## 3. The mixed problem for unit circle

This part sums up the main results (for more details see Mushkelishvili [18] and Gakhov [19]). For further explanations about numerical treatment of this boundary problem, see Legallais, Hureau and Brunon [14].

Let $L$ be the unit circle, and $S^+$ the unit disk bounded by $L$. The complement of $S^+$ is the infinite region $S^-$, $a_1b_1, a_2b_2, \ldots, a_pb_p$ are disconnected arcs on the contour $L$. Arcs $a_jb_j$ will be denoted by $L'$, and arcs $b_ja_{j+1}$ by $L''$ (*figure 3*).

The aim of the mixed problem for the unit circle is to determine the function $\phi(z) = \varphi + i\psi$, such that the boundary conditions

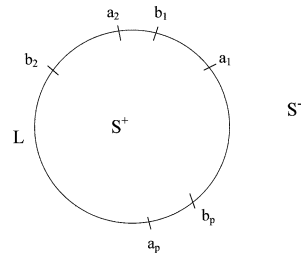


**Figure 3.** Unit circle and unit disk.

$$\varphi^+ = f_1(t) \quad \text{on } L',$$
$$\psi^+ = f_2(t) \quad \text{on } L''$$

hold ($f_1$ and $f_2$ are given functions). The solution is then unique and has the form:

$$\phi(z) = \frac{X(z)}{i\pi} \int_L \frac{c(t)\,\mathrm{d}t}{[a(t) + ib(t)]X^+(t)(t-z)}$$

with

$$X(z) = \sqrt{\prod_{j=1}^{P}(z-a_j)(z-b_j)} \quad (X^+ \text{ being the restriction of } X \text{ in } S^+)$$

and

$$a(t) = 1,\ b(t) = 0,\ c(t) = f_1(t) \quad \text{on } L',$$
$$a(t) = 0,\ b(t) = -1,\ c(t) = f_2(t) \quad \text{on } L''.$$

In this paper we are concerned with the two-arc mixed problem, which consists of calculating the real part of an analytical function $\phi$ on $L''$ and its imaginary part on $L'$. Its imaginary part is given on $L''$ and its real part on $L'$. The solution may be rewritten in the form:

$$\phi(z) = \frac{X(z)}{\pi} \int_{L''} \frac{f_2(t)}{X^+(t)(t-z)}\,\mathrm{d}t + \frac{X(z)}{i\pi} \int_{L'} \frac{f_1(t)}{X^+(t)(t-z)}\,\mathrm{d}t, \tag{1}$$

with

$$X(z) = \sqrt{(z-1)(z+1)}.$$

After some algebraic transformations, this becomes:

- $z = \mathrm{e}^{i\alpha}$ on the boundary $L$

$$\phi(z) = \frac{\sqrt{\sin\alpha}}{2\pi\sqrt{2}} \left[ \int_0^{\pi} \frac{f_2(\mathrm{e}^{i\sigma})\,\mathrm{d}\sigma}{\sqrt{\sin\frac{\sigma}{2}}\sqrt{\cos\frac{\sigma}{2}}\sin\frac{\sigma-\alpha}{2}} + \int_{\pi}^{2\pi} \frac{f_1(\mathrm{e}^{i\sigma})\,\mathrm{d}\sigma}{\sqrt{\sin\frac{\sigma}{2}}\sqrt{-\cos\frac{\sigma}{2}}\sin\frac{\sigma-\alpha}{2}} \right], \quad \alpha < \pi,$$

$$\phi(z) = -i\frac{\sqrt{-\sin\alpha}}{2\pi\sqrt{2}} \left[ \int_0^{\pi} \frac{f_2(\mathrm{e}^{i\sigma})\,\mathrm{d}\sigma}{\sqrt{\sin\frac{\sigma}{2}}\sqrt{\cos\frac{\sigma}{2}}\sin\frac{\sigma-\alpha}{2}} + \int_{\pi}^{2\pi} \frac{f_1(\mathrm{e}^{i\sigma})\,\mathrm{d}\sigma}{\sqrt{\sin\frac{\sigma}{2}}\sqrt{-\cos\frac{\sigma}{2}}\sin\frac{\sigma-\alpha}{2}} \right], \quad \alpha > \pi,$$

- $z = \rho\,\mathrm{e}^{i\alpha}(\rho < 1)$ in $S^+$

$$\phi(z) = \frac{i\sqrt{z^2-1}}{\pi\,\mathrm{e}^{i\frac{\pi}{4}}}\left[\int_0^{\pi} \frac{c(\mathrm{e}^{i\sigma})\mathrm{e}^{i\frac{\sigma}{2}}\,\mathrm{d}\sigma}{\sqrt{2\sin\sigma}(\mathrm{e}^{i\sigma}-z)} + \int_{\pi}^{2\pi} \frac{c(\mathrm{e}^{i\sigma})\mathrm{e}^{i\frac{\sigma}{2}}\,\mathrm{d}\sigma}{\sqrt{-2\sin\sigma}(\mathrm{e}^{i\sigma}-z)}\right].$$

Note that this type of boundary problem has been solved theoretically on the half plane; however, from a numerical point of view, the integrals are complicated by the infinite range of integration (see Peng and Parker [12]).

## 4. Mathematical formulation and numerical method

### *4.1. OCF*

As the mixed problem was numerized in Section 3 with the imaginary part of the unknown function given on the upper half of the unit circle, the function $Q$ will be reserved for OCF.

$$Q = i\,\mathrm{Log}\frac{V_{\mathrm{ref}}}{w} = T(\zeta) + i\Theta(\zeta)$$

on the unit circle, $\zeta = \mathrm{e}^{i\sigma}$ and $Q = \tau(\sigma) + i\theta(\sigma)$.

According to the expression for the different conformal mappings, and using $z = \int \frac{\mathrm{d}f}{w}$, it follows that:

$$\mathrm{d}f = -2\frac{V_{\mathrm{A}}H}{\pi}\frac{\mathrm{d}\zeta}{(1+\zeta)(1-\zeta)} \quad \text{and} \quad \mathrm{d}z = \frac{-2H}{\pi}\frac{V_{\mathrm{A}}}{V_{\mathrm{ref}}}\frac{\mathrm{e}^{T(\zeta)}\,\mathrm{e}^{i\Theta(\zeta)}}{(1+\zeta)(1-\zeta)}\,\mathrm{d}\zeta, \tag{2}$$

$$\mathrm{d}f = \frac{V_{\mathrm{A}}H}{\pi}\frac{\mathrm{d}\sigma}{\sin\sigma} \quad \text{and} \quad \mathrm{d}z = \frac{H}{\pi}\frac{V_{\mathrm{A}}}{V_{\mathrm{ref}}}\frac{\mathrm{e}^{\tau(\sigma)}\,\mathrm{e}^{i\theta(\sigma)}}{\sin\sigma}\,\mathrm{d}\sigma. \tag{3}$$

From (2) and (3), we have obvious reasons for taking $V_{\mathrm{ref}} = V_{\mathrm{A}}$.

To calculate $Q$, we have to solve the mixed problem described in Section 3. From now on, we will call (as in Section 3) $L''$ the upper-half circle in $D_\zeta$ and $L'$ the lower one.

Let $\beta$ be the angle between the tangent at a point on the wetted wall and the $x$-axis. It follows that $\theta = \beta(s)$, which leads us to introduce $\varepsilon$, the one-to-one correspondence function between the walls of $D_\zeta$ and $D_z$:

$$\varepsilon\colon\ \sigma \in [0,\pi] \mapsto s = \varepsilon(\sigma), \quad s \in\, ]-\infty, +\infty[$$

then, on $L''$,

$$\theta(\sigma) = \beta\big(\varepsilon(\sigma)\big). \tag{4}$$

Bijection $\varepsilon$ is obtained by integrating $\mathrm{d}s = |\mathrm{d}z|$ from (3):

$$\varepsilon(\sigma) = \frac{H}{\pi}\int_{\pi/2}^{\sigma} \frac{\mathrm{e}^{\tau(\sigma')}}{\sin\sigma'}\,\mathrm{d}\sigma'. \tag{5}$$

The missing data needed to solve the mixed problem is $\tau$. It can be easily obtained from the Bernoulli's equation.

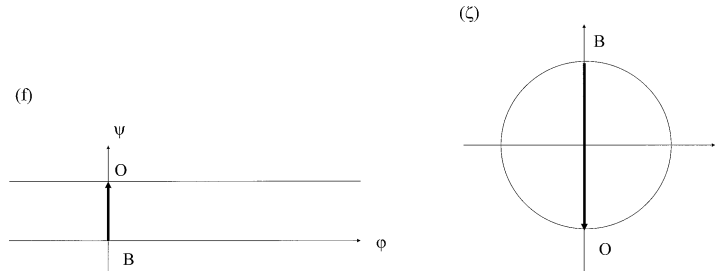


**Figure 4.** The location of point O.

*4.1.1. Weightless fluid*

$|w| = V_A$ which leads to

$$\tau(\sigma) = 0. \tag{6a}$$

Then, solving the mixed problem gives us $\tau(\sigma)$ on $L''$ and $\theta(\sigma)$ on $L'$.

The functional system has the form:

$$\begin{aligned} \tau &= G_1(\theta, \tau), \\ \theta &= G_2(\theta, \tau), \\ \varepsilon &= G_3(\tau). \end{aligned}$$

In order to solve this system, a sequence $\{\varepsilon_n, \tau_n, \theta_n\}$ is constructed by means of the relaxed iterative algorithm detailed below.

$$\begin{aligned} \tau_n &= G_1(\theta_{n-1}, \tau_{n-1}), \\ \theta_n &= G_2(\theta_{n-1}, \tau_{n-1}), \\ \varepsilon_n &= (1 - r_\varepsilon)G_3(\tau_n) + r_\varepsilon \varepsilon_{n-1}, \end{aligned}$$

where $r_\varepsilon$ is a weighting factor varying between 0 and 1.

The initial data is $H$, the height of the flow far upstream (*figure 1*). An arbitrary correspondence $\varepsilon(\sigma)$ is chosen, giving $\theta(\sigma)$ on $[0, \pi]$ by (4), whereas $\tau(\sigma)$ is given on $[\pi, 2\pi]$ by (6a). We get the complementary values of $\tau(\sigma)$ on $[0, \pi]$ and $\theta(\sigma)$ on $[\pi, 2\pi]$ from the solution (1) of the mixed problem and a new function $\varepsilon$ may be obtained by (5). When convergence is reached, the process is stopped by a test on the relative error associated with unknown $\varepsilon$. Then we can get the free surface AC. This is done by considering the equipotential BO ($\phi = 0$) in $D_f$, which gives the location of point O, defined in *figure 4*.

$$z_O = z_B + \frac{H}{\pi} \int_i^{-i} \left( \frac{1}{\zeta - 1} - \frac{1}{\zeta + 1} \right) e^{i\Theta(\zeta)} e^{T(\zeta)} \, d\zeta. \tag{7}$$

Then both lines OA and OC derive from (3):

$$z = z_O + \frac{H}{\pi} \int_{3\pi/2}^{\sigma} \frac{e^{i\theta(\sigma)} e^{\tau(\sigma)}}{\sin \sigma} \, d\sigma. \tag{8}$$

*4.1.2. Heavy fluid*

$$\frac{1}{2}\rho V_{\mathrm{A}}^2 + \rho g H = \frac{1}{2}\rho |w|^2 + \rho g y,$$

which leads to

$$\tau(\sigma) = -\frac{1}{2}\log\left[1 + \frac{2}{F^2}\left(1 - \frac{y(\sigma)}{H}\right)\right]. \tag{6b}$$

Equation (6b) implies additional work in a heavy fluid: the free surface AC has to be calculated at each iteration to determine $y$ and then $\tau$. This is done by equations (7) and (8).

The initial data are $H$ and $F$ the Froude number far upstream. However, the results already published concerning this study indicate that there can be two solutions for a given couple $(F,\ H)$ (see next paragraph). So we have to choose another parameter in order to differentiate these solutions. We introduce therefore $Y_{\mathrm{O}}$, the height of point O introduced previously, as an additional datum. It must be noted that for an arbitrary given series $(F,\ H,\ Y_{\mathrm{O}})$ there can be no solution to the problem, since once two of them are imposed, the third is no longer a parameter.

An arbitrary correspondence $\varepsilon(\sigma)$ and free surface AC are chosen, giving respectively $\theta(\sigma)$ by (4) and $\tau(\sigma)$ by (6b). We get the complementary values of $\tau(\sigma)$ and $\theta(\sigma)$ from the resolution of the mixed problem (1). A new function $\varepsilon$ is obtained by (5). The new values of $\tau(\sigma)$ on $[\pi, 2\pi]$ are obtained by building the free surface AOC by (7) and (8), and translating it vertically, so that the height of point O corresponds to $Y_{\mathrm{O}}$.

When convergence is reached, the process is stopped as previously. Then we compare the heights of point O and A with respectively $Y_{\mathrm{O}}$ and $H$, to see whether this convergence does represent a solution.

Our method offers three major advantages:

- Any curved wall can be computed (its equation known or unknown);
- Any initial arbitrary guess for $\varepsilon$ and $\tau$ will do to obtain a solution (more will be said about this in Section 4);
- It can consider either weightless fluid or heavy fluid. However, in the case of heavy fluid, Forbes [17] showed that this type of resolution can only deal with supercrititical flows.

When the bottom of the channel contains one or more corners, $w$ and $Q$ exhibit singularities:

– the real part of $Q$ is infinite;
– the imaginary part of $Q$ jumps by $\delta\pi$ (if we call $\delta\pi$ the jump of the tangent at one corner).

To express these singularities we introduce another function called $Q_{\mathrm{S}}$ having the same singularities as $Q$. This way, we isolate the singularity by writing $Q = Q_{\mathrm{S}} + \widetilde{Q}$, and this comes down to considering the function $\widetilde{Q}$ instead of $Q$, to be continuous in both its real and imaginary parts.

The function

$$Q_{\mathrm{S}} = -\mathrm{Log}\left(\zeta - \mathrm{e}^{i\gamma}\right)^{\delta} \tag{9}$$

has the required singularities.

Equation (9) leads to:

$$\widetilde{\tau} = \tau + \delta \log\left|2\sin\frac{\gamma - \sigma}{2}\right|,$$

$$\widetilde{\theta} = \theta + \delta\left(\frac{\gamma + \sigma}{2} + \frac{3\pi}{2}\right), \quad \sigma < \gamma, \qquad \widetilde{\theta} = \theta + \delta\left(\frac{\gamma + \sigma}{2} + \frac{\pi}{2}\right), \quad \sigma > \gamma.$$

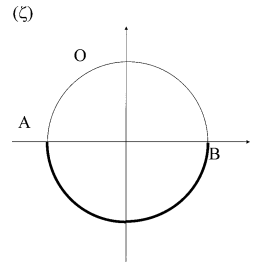


**Figure 5.** The ($\zeta$)-plane for the WF case.

For this method we need to know $\gamma$, which is the argument of the homologue of the singularity in $D_\zeta$. Since the corner position $s_\gamma$ is known in the physical plane, $\gamma$ is deduced as soon as $\varepsilon$ is computed. The mixed problem considers $\widetilde{Q}$ instead of $Q$; otherwise the solution sequence is unchanged.

### *4.2. WF*

We do not detail this study, since it is similar to the previous one. We just consider in this case another ($\zeta$)-plane, *figure 5*, and function $\Omega = i\,\mathrm{Log}\frac{w}{V_{\mathrm{ref}}} = \Theta(\zeta) + iT(\zeta)$ instead of $Q$. Equations (2), (3), (5) and (6b) now become:

$$\mathrm{d}z = \frac{2H}{\pi}\,\frac{V_{\mathrm{A}}}{V_{\mathrm{ref}}}\,\frac{\mathrm{e}^{-T(\zeta)}\,\mathrm{e}^{i\Theta(\zeta)}}{(1+\zeta)(1-i)(i-\zeta)}\,\mathrm{d}\zeta, \tag{2′}$$

$$\mathrm{d}z = \frac{H}{\pi}\,\frac{V_{\mathrm{A}}}{V_{\mathrm{ref}}}\,\frac{\mathrm{e}^{-\tau(\sigma)}\,\mathrm{e}^{i\theta(\sigma)}}{1+\cos\sigma-\sin\sigma}\,\mathrm{d}\sigma, \tag{3′}$$

$$\varepsilon(\sigma) = \frac{H}{\pi}\int_{2\pi}^{\sigma}\frac{\mathrm{e}^{-\tau(\sigma')}}{1+\cos\sigma'-\sin\sigma'}\,\mathrm{d}\sigma', \tag{5′}$$

$$\tau = \frac{1}{2}\log\left[1+\frac{2}{F^2}\left(1-\frac{y}{H}\right)\right]. \tag{6b′}$$

## 5. Computed results

### *5.1. OCF*

#### *5.1.1. Obstacle lying on a flat bottom*

From now on, we will call $h$ the height of the obstacle.

*Solution existence*:

For a given obstacle and a given ratio $h/H$, there is one Froude number, or for a given Froude number there is one ratio $H/h$, below which no solution to this problem exists. Moreover, there is a flow configuration where the free-surface reaches its maximum elevation, corresponding to a stagnation point. It can then be written $|w| = 0$, and from (5) (heavy fluid), $1 + \frac{2}{F^2}(\frac{y_{\mathrm{A}}-y}{H}) = 0$, and so $y_{\mathrm{stagnation}} = y_{\mathrm{A}} + \frac{F^2}{2}H$. This stagnation point is characterized by a 120° corner.

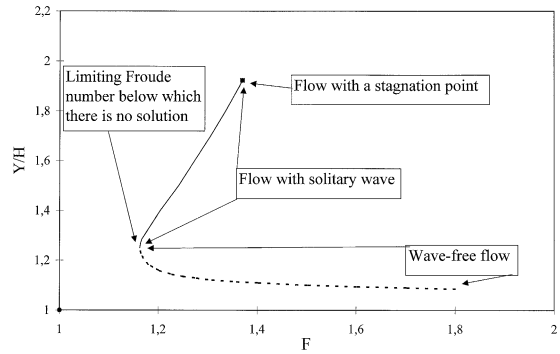


**Figure 6.** The different flow types in supercritical far upstream flows.

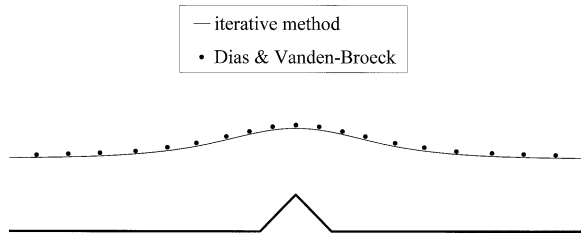


**Figure 7.** Comparison between the iterative method (this article) and [6]; the Froude number is 1.43 and the ratio $h/H$ equals 0.5.

We present in *figure 6* the different flows that can be encountered in supercritical far upstream flows. The curve represents a given ratio $h/H$.

Before applying this method to arbitrary flows, we tested it by comparison with previously published results.

*Triangular obstacle*:

A computation has been performed (*figure 7*) and compared with Dias and Vanden-Broeck's results [6]. Our results show small differences. These differences come from the simple geometry of wall in *figure 7*. Indeed, the variable $\theta$ exhibits only four values in $D_\zeta$ ($0, \pi/4, -\pi/4$ and 0 from A to C on the upper semi-circle), and as it has been shown in [15], our method has in this case some difficulties to find accurately the solution of the problem. On the other hand, when this variable $\theta$ is not constant (see following sections), our results show very good agreement with those already published.

*Semi-circular obstacle*:

Our program has calculated some of the results already established by Forbes and Schwartz [4], for a semi-circular obstacle (*figure 8*). The free surface obtained reproduces theirs closely. The same agreement is obtained when the Froude number varies.

A similar comparison has been performed with Vanden-Broeck's results [5] (*figure 9*).

The following graph shows $Y/H$ ($Y$ is the maximum height of the free surface) as a function of the Froude number $F$, for three ratios $h/H$ (*figure 10*). As for Vanden-Broeck's results, the non-uniqueness of the solution at a given Froude number clearly appears.

*Curved walls*:

Here are two flows already computed by King and Bloor [10] (*figure 11*). The equation of the wall is given and gravity is not taken into account. We can see the very good agreement between our results and theirs.

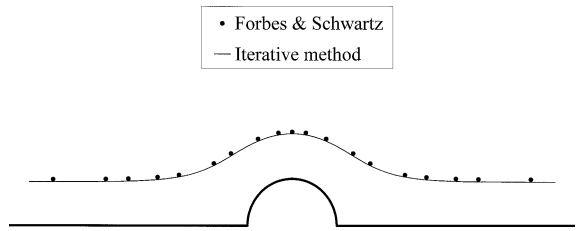


**Figure 8.** Comparison between the iterative method (this article) and [4]; the Froude number is 2.1 and the ratio $h/H$ equals 1.1.

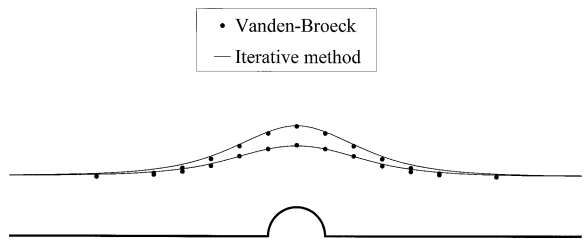


**Figure 9.** Comparison between the iterative method (this article) and [10]; the Froude number is 1.48 and the ratio $h/H$ equals 0.5.

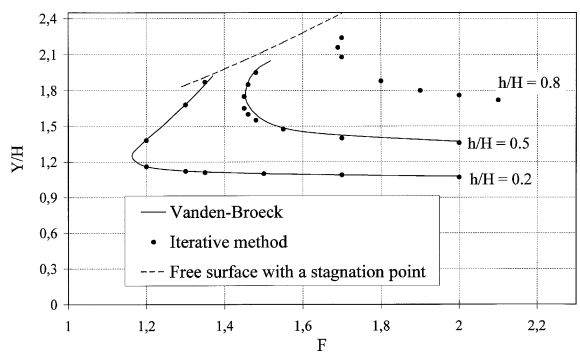


**Figure 10.** Ratio $Y/H$ function of the Froude number for a semi-circular obstacle.

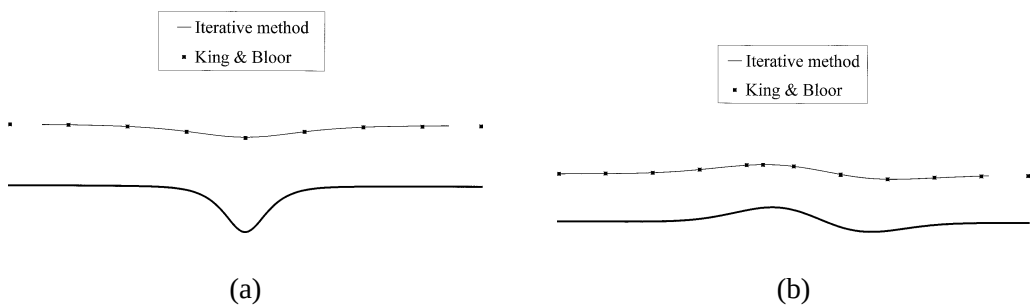


**Figure 11.** Comparison between the iterative method (this article) and [10]; the equation of the wall is left: $y = -1.5/(\exp(\pi x) + \exp(-\pi x))$; right: $y = 0.5 \cdot \exp(-x^2/2) - 0.4 \cdot \exp(-0.5 \cdot (x-1)^2)$.

Next we present three arbitrary obstacles (*figure 12*), the last one being more complicated to show the ability of our method.

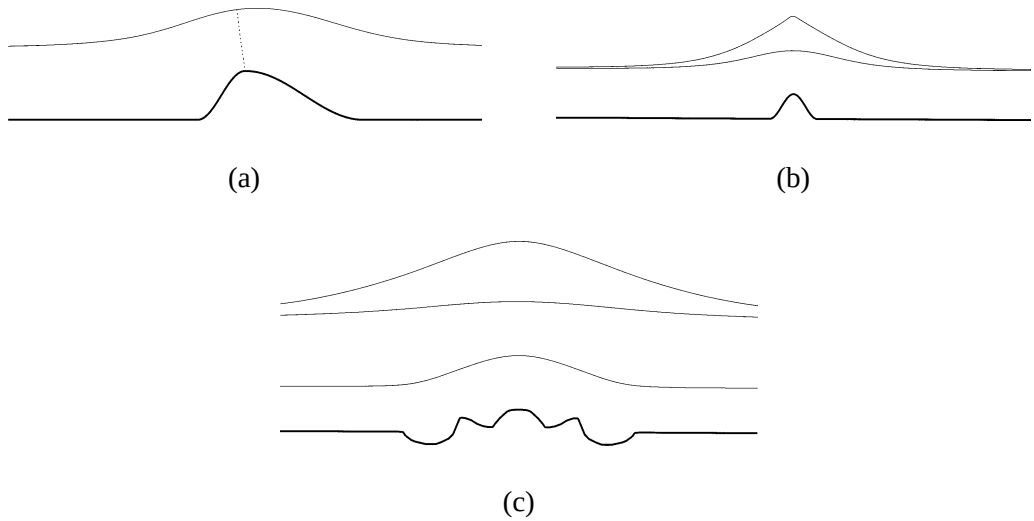


**Figure 12.** An arbitrary obstacle; (a) the Froude number is 2.2 and the ratio $h/H$ equals 0.667. The equipotential BO is indicated by short-dashed line; (b) the Froude number is 1.5 and the ratio $h/H$ equals 0.5; (c) The Froude number is 2.0 and the ratio $h/H$ equals 0.5 (lower curve); the Froude number is 1.3 and the ratio $h/H$ equals 0.2 (upper curves).

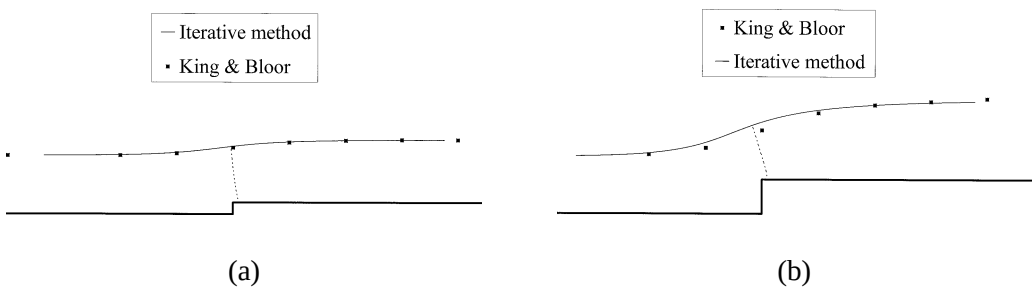


**Figure 13.** Comparison between the iterative method (this article) and [9]; (a) $h/H = 0.2$; (b) $h/H = 0.6$.

These comparisons show that this method can solve the problem of the flow of a heavy fluid over a flat bottom with an arbitrary obstacle. As a generalization, we are now going to consider the flow over an arbitrary shaped bottom, this last case being not found in the literature.

*5.1.2. Arbitrary shaped bottom*

First we compare our results with the only ones found, those obtained by King and Bloor [9] (*figure 13*), concerning the flow over a step. In both figures, the Froude number is 2. The equipotential BO is indicated in short-dashed line. We can see some little discrepancies between these comparisons. The reason is probably the same as before, since the variable $\theta$ has only three values in this case: 0, $\pi/2$ and 0. An additional mistake may come from the reading of King and Bloor's results, since the free surface was presented in a figure with a very small scale in the O$x$ axis.

With our iterative method, any supercritical flow of a heavy fluid over arbitrary walls can be computed, such as these presented *figure 14* (the short-dashed line corresponds to the equipotential BO and the broken line to the weightless fluid).

We emphasize the fact that these results were obtained regardless of the initial guesses, which shows that our method seems to be very insensitive with regard to them.

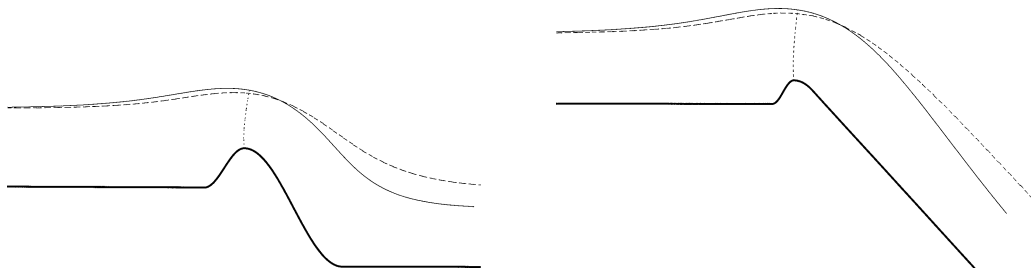

(a) (b)

**Figure 14.** Supercritical flow of a heavy fluid over arbitrary walls; (a) the Froude number is 1.6 and the ratio $h/H$ equals 0.5; (b) the Froude number is 1.7 and the ratio $h/H$ equals 0.333.

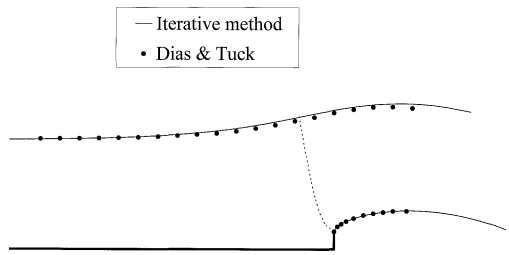


**Figure 15.** Comparison between the iterative method (this article) and [7]; the Froude number is 1.66 and the ratio $h/H$ equals 0.16. The horizontal scale is the same as the vertical scale.

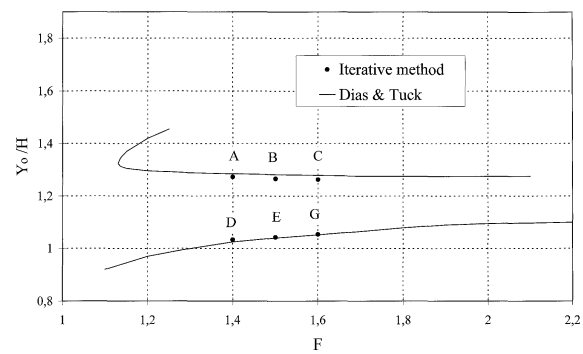


**Figure 16.** Ratio $Y_O/H$ function of the Froude number for a horizontal bottom ending by a vertical wall.

### *5.2. WF*

For a horizontal bottom ending by a vertical wall the results are in good agreement with those published by Dias and Tuck [7] (*figure 15*).

Next, as for OCF, we present the ratios $Y_O/H$ ($Y_O$ being the height of point O) et $Y/H$ ($Y$ being the maximal height of the free-surface) function of the Froude number (*figures 16* and *17*). Results by Dias and Tuck [7] correspond to curves where one of their parameters is constant. This parameter being different from the ratio $h/H$ in *figure 6*, we indicate the values of this ratio for the flows noted from A to G.

– Flows A: $h/H = 0.1923$, B: $h/H = 0.1961$, C: $h/H = 0.2000$;

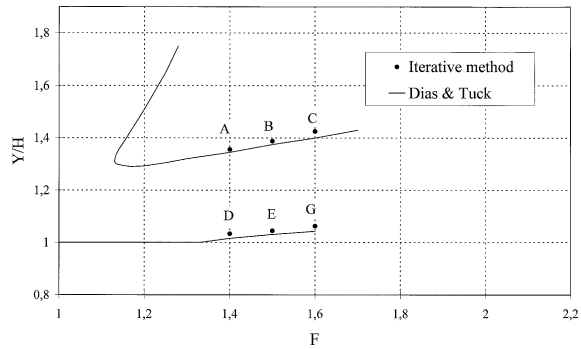


**Figure 17.** Ratio $Y/H$ function of the Froude number for a horizontal bottom ending by a vertical wall.

– Flows D: $h/H = 0.0571$, E: $h/H = 0.0556$, G: $h/H = 0.0556$.

This is the only comparison we were able to make for a waterfall, since no other supercritical wave-free flow has been found in the literature.

Next, we show a series of results obtained on two arbitrary bottoms, with different Froude numbers (*figures 18, 19* and *20*)). The first one represents a whimsical shape, whose hydrodynamical importance is limited, chosen to show the ability of our method. The equipotential BO is indicated in each figure by the short-dashed line and the horizontal scale is the same as the vertical scale.

As was said above, there is a limiting configuration, depending on the choice of $V_A$ and $H/h$ from which, if these values are decreased, there is no solution to the flow. *Figures 20(a)* and *20*(*b*) represent the limiting configuration we were able to calculate. This corresponds to a similar point presented in *figures 16* and *17*, where the curve folds back over itself.

Convergence is obtained after 10 or 20 iterations, requiring a few minutes of calculation on a PC Pentium 100 MHz computer.

## 6. Numerical quadrature

### *6.1. OCF*

A regular distribution was used on the $[1°,\ 179°]$ arc, with 300 points. An irregular distribution (about 10 points) was required on the two arcs $[0°,\ 1°]$ and $[179°,\ 180°]$, in order to go as far as possible in the vicinity of A and C corresponding to the wall. On the free surface AOC, 300 points were used, regularly distributed on each arc $[181°,\ 270°]$ and $[359°,\ 270°]$, plus 25 irregular points near A (arc $[359°,\ 360°]$) and C (arc $[180°,\ 181°]$), in order to trace the free surface far enough.

The effect of the discretisation appears in *figure 21*. *Figure 21*(*a*) presents the solution obtained with the above described discretisation, whereas *figure 21*(*b*) is the solution obtained with only 2 points (instead of 25) on the arcs $[180°,\ 181°]$ and $[359°,\ 360°]$. In the former case, the last point indicated on the free-surface AC is only $1.9.10^{-6}$ degree away from point C in the $(\zeta)$-plane; in the latter case it is 0.5 degree away. However, in both cases, the common part is the same, which means that the solution does not seem to depend on the discretisation.

It has only to be kept in mind that the computational points around the domain must not be more than 1 degree apart, otherwise significant errors begin to appear in the mixed problem when digitized.

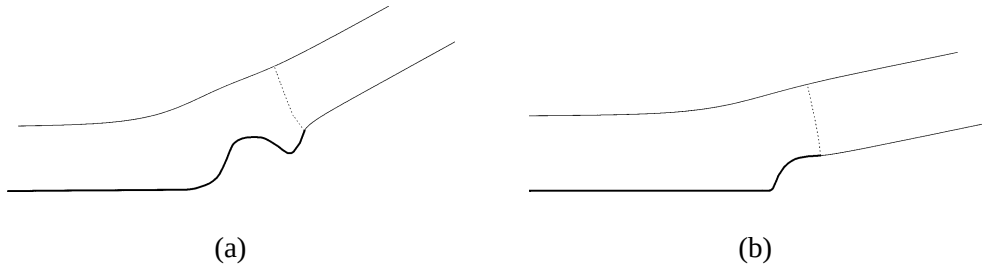


**Figure 18.** Flows over 2 arbitrary bottoms; the Froude number is $+\infty$ (weightless fluid).

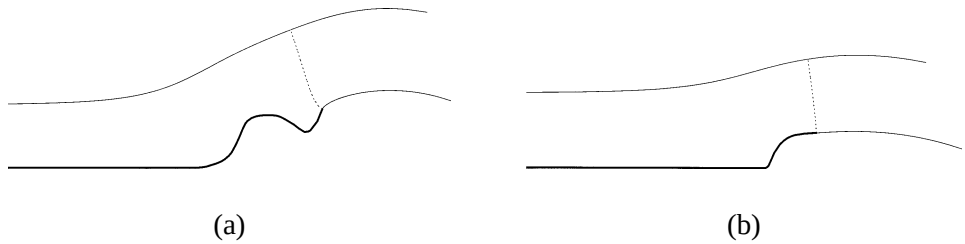


**Figure 19.** As *figure 18*; the Froude number is 2.258.

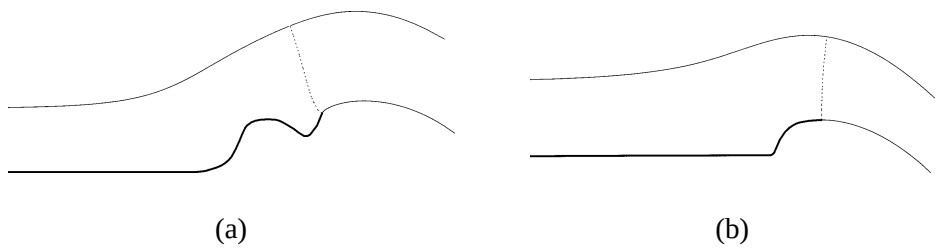


**Figure 20.** As *figure 18*; the Froude number is 2.032 (left), and 1.408 (right).

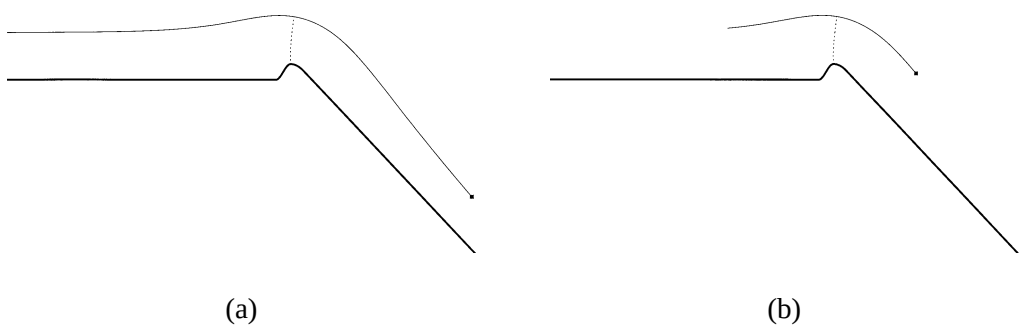


**Figure 21.** The effect of discretisation.

### *6.2. WF*

A constant division (350 points) was used on the [182°, 360°] arc, plus an irregular division on the arc [180°, 182°] (40 points). To trace the jet BC, 180 regular points were chosen on the [0°, 89°] arc, and

20 irregular points were added on the [89°, 90°] arc, to trace the line BC as far as possible. Finally, a regular distribution was used on the [90°, 178°] arc (180 points), plus 40 irregular points near A (arc [178°, 180°]).

To trace the equipotential BO, 100 points were chosen in both cases.

## 7. Conclusion

According to the results obtained, we believe that now the free-surface flow over an arbitrary bottom can be clearly computed, both for open channel flow and for a waterfall configuration. Its only limitation is the usual crowding due to conformal mapping, which prevents us from taking into account a length of flow stretching for more than five or ten heights. So we can consider one or more deformations of the wall, if they are close enough (see *figures 18, 19* and *20*). Otherwise we have to treat several flow problems separately. Despite this crowding, the free surfaces far downstream can be drawn far enough by using many quadrature points in the vicinity of C in the $\zeta$ plane.

In this method, the fluid is assumed to be heavy and inviscid, which is a tolerable assumption here since the part of the flow we investigate is short enough to neglect loss of head. For this reason, we believe the results we obtain rapidly give a fairly good description of the real flow.

## Acknowledgments

We would like to thank F. Dias for his remarks about the results presented in this paper, and particularly to have incited us to carry on with our research in order to find the solitary-wave-type solutions.

## References

[1] Kirchhoff G., Zur Theorie freier Flüssigkeitsstrahlen, J. Reine Angew. Math. 70 (1869) 289–298.
[2] Gurevich M.I., The theory of jets in an ideal fluid, Pergamon Press, Oxford, 1966.
[3] Dias F., Elcrat A.R., Trefethen L.N., Classical free streamline flow over a polygonal obstacle, J. Comput. Appl. Math. 14 (1986) 251–265.
[4] Forbes L.K., Schwartz L.W., Free-surface flow over a semi-circular obstruction, J. Fluid Mech. 114 (1982) 299–314.
[5] Vanden-Broeck J.-M., Free-surface flow over an obstruction in a channel, Phys. Fluids 30 (1987) 2315–2317.
[6] Dias F., Vanden-Broeck, J.-M., Open channel flows with submerged obstructions, J. Fluid Mech. 206 (1989) 155–170.
[7] Dias F., Tuck E.O., Weir flows and waterfalls, J. Fluid Mech. 230 (1991) 525–539.
[8] Bloor M.I.G., Large amplitude surface waves, J. Fluid Mech. 84 (1978) 167–179.
[9] King A.C., Bloor M.G.I., Free-surface flow over a step, J. Fluid Mech. 182 (1987) 193–208
[10] King A.C., Bloor M.G.I., Free streamline flow over curved topography, Q. Appl. Math. XLVIII (2) (1990) 281–293.
[11] King A.C., Bloor M.G.I., Free-surface flow of a stream obstructed by an arbitrary bed topography, J. Comput. Appl. Math. 43 (1990) 87–106.
[12] Peng W., Parker D.F., An ideal fluid jet impinging on an uneven wall, J. Fluid Mech. 333 (1997) 231–255.
[13] Hureau J., Mudry M., Nieto J.L., Une méthode générale d'écoulements avec sillages de Helmholtz, C. R. Acad. Sci. II 305 (1987) 331–334.
[14] Legallais Ph., Hureau J., Brunon E., Determination of flows past curved obstacles with wakes using a mixed problem solution, Eur. J. Mech. B-Fluids 14 (1995) 275–299.
[15] Hureau J., Brunon E., Legallais Ph., Ideal free streamline flow over a curved obstacle, J. Comput. Appl. Math. 72 (1996) 193–214.
[16] Hureau J., Weber R., Impinging free jets of ideal fluid, J. Fluid Mech. 372 (1998) 357–374.
[17] Forbes L.K., Irregular frequencies and iterative methods in the solution of steady surface-wave problems in hydrodynamics, J. Eng. Math. 18 (1984) 299–313.
[18] Muskhelishvili N.I., Singular integral equations, Noordhoff International Publishing, 1977.
[19] Gakhov F.D., Boundary Value Problems, Pergamon Press, Oxford, 1966.